

Constant voltage control of a secondary side controlled wireless power transfer converter using LC/S compensation

LC/S kompanzasyonu kullanan sekonder taraf kontrollü bir kablosuz güç transfer dönüştürücüsünün sabit gerilim kontrolü

Veli YENİL¹ , Sevilay ÇETİN^{2*} 

¹Cardak Organized Industrial Regional Vocational High School, Pamukkale University, Denizli, Turkey.
veliyenil@pau.edu.tr

²Department of Biomedical Engineering, Technology Faculty, Pamukkale University, Denizli, Turkey.
sctin@pau.edu.tr

Received/Geliş Tarihi: 09.03.2021
Accepted/Kabul Tarihi: 02.11.2021

Revision/Düzelme Tarihi: 24.10.2021

doi: 10.5505/pajes.2021.99390
Research Article/Araştırma Makalesi

Abstract

In this study, constant voltage control of a secondary side controlled wireless power transfer (WPT) converter is evaluated based on efficiency. The LC/S compensation network which has perfect constant current characteristic is used in the design of the WPT converter. In order to improve the constant voltage performance of the LC/S compensation network, controlled rectifier is adapted to the converter. The phase shift modulation (PSM) control is applied to the switches of the rectifier as independent of the primary side. Thus, constant voltage regulation is achieved at constant operation frequency in a wide load range. The performance of the proposed converter is verified by a simulation work at 2.5 kW output power and 450 V output voltage. The efficiency values of the converter, as function of the load condition, is extracted by simulation and compared to frequency modulation control. In addition, power loss distribution and its comparison with frequency modulation is also discussed. The maximum efficiency of the converter is obtained 96.4% at full load condition.

Keywords: Wireless power transfer, Constant voltage control, Efficiency, Battery charging.

Öz

Bu çalışmada, sekonder taraf kontrollü bir kablosuz güç aktarım (WPT) dönüştürücüsünün sabit gerilim kontrolü, verime dayalı olarak değerlendirilmiştir. WPT dönüştürücüsünün tasarımında güçlü sabit akım karakteristiğine sahip LC/S kompanzasyon topolojisi kullanılmıştır. LC/S kompanzasyon topolojisinin sabit gerilim performansını iyileştirmek için, kontrollü doğrultucu dönüştürücüye uyarlanmıştır. PSM kontrolü doğrultucu anahtarlarına primer taraftan bağımsız olarak uygulanmıştır. Böylece, geniş bir yük aralığında sabit çalışma frekansında sabit gerilim regülasyonu elde edilir. Sunulan dönüştürücüsünün performansı, 2.5 kW çıkış gücü ve 450 V çıkış geriliminde simülasyon çalışmasıyla doğrulanmıştır. Yük durumunun fonksiyonu olarak dönüştürücüsünün verim değerleri simülasyon ile çıkarılmış ve frekans modülasyonu ile karşılaştırılmıştır. İlaveten, güç kaybı dağılımı ve frekans modülasyonu ile karşılaştırması incelenmiştir. Dönüştürücüsünün maksimum verimi, tam yük durumunda %96.4 olarak elde edilmiştir.

Anahtar kelimeler: Kablosuz enerji transferi, Sabit gerilim kontrolü, Verim, Batarya şarjı.

1 Introduction

Nowadays, wireless power transfer (WPT) method is very popular because the isolation between the source and the load provides high level safety. In addition, the weather proof feature provides comfort and reliability. WPT is used in a wide variety of industrial applications such as high-power electric vehicles, low power consumer electronics and biomedical implants [1]-[3]. In the battery charging applications, Lithium-ion batteries which is providing high power density and long cycle life [4],[5] is very common. In order to provide safe charging process of the Lithium-ion battery, the constant current (CC) and the constant voltage (CV) charge control modes should be implemented [6].

The low coupling between primary and secondary coils of the WPT system is well known problem. The air gap between coils causes large leakage inductance and reactive power in the system. Therefore, compensation networks are used to compensate the reactive power and increase the power transfer efficiency [7]. The conventional compensation networks can achieve compensation function with the additional two capacitors, so they have simple structure, low

power loss and provide cheap solution [8]-[12]. However, they can provide load independent CC or CV output, which are dependent of the parameters of the coils [13], [14]. Parallel compensation of the primary side provides only CC or CV [14]. Series-series (SS) and series-parallel (SP) compensation networks provide load independent CC and CV output, respectively. The zero phase angle (ZPA) and zero voltage switching are also achieved as load independent. However, SS compensation network lost ZPA operation during CV control operation. Similarly, SP compensation cannot maintain ZPA during CC control operation. The operation frequency has to be changed to achieve required CC or CV output. Thus, an increase in reactive power causes a decrease in efficiency. The conventional compensation networks are not qualified for entire charge period of the battery [15]-[17].

The hybrid topologies providing CC and CV control of the WPT system are exist in the literature. In the many applications, LC/L and LCC compensation networks are usually preferred because of their benefits. The LC/L compensation network is needed additional inductors to primary and secondary sides. These inductors require design optimization based on power balance inverter and compensation network [18]. In [19], additional

*Corresponding author/Yazışılan Yazar

inductors of the LC/L compensation network are very large, which results in low system efficiency.

In [20], circulating current of the receiver coil is reduced with the addition of an LC circuit to parallel compensation in secondary side. However, an additional inductor increases the size and cost of the system. The LCC compensation network uses additional capacitor instead of additional inductor of LC/L compensation [21]. The zero current switching (ZCS) of the inverter switches is achieved in the proposed work. A double sided LCC compensation network achieves the zero voltage switching (ZVS) turn-on of the inverter switches and its maximum power point is independent of load condition [22]. Besides, eliminating of additional inductor provides higher efficiency compared to LC/L compensation. However, four capacitors and two inductors of the network cause too many circuit elements. In [23], an LC/S compensation network, providing good CC characteristic, is presented. According to given results, efficiency of the LC/S compensation is very close to the double sided LCC compensation network, by the use of less number of circuit component. However, proposed design procedure cannot achieve the load independent CV control. In [24], another design procedure of LC/S compensation provides CV operation. The presented design procedure is complex and CC control operation is not evaluated.

The CC and CV charging period of the WPT system can be achieved with the variation of the operation frequency [15], [16],[25]. The frequency change can handle the output regulation while the reactive power of the system is increased, and power transfer efficiency is reduced. The additional converter connected to the rectifier is another way to regulate the output instead of frequency variation [26],[27]. However, additional converter results in large volume, extra power losses and high cost.

The use of controlled rectifier can allow voltage regulation by the set of the effective resistance seen at input of the rectifier. A dual side controlled WPT system is proposed in [28]. The load condition and coupling factor variation of the proposed system are evaluated with the control of dual side. The requirement of the communication of primary and secondary side makes the controller design complex. A phase shift control method applied to the semi bridgeless active rectifier (SBAR) eliminates the need of communication of dual side [29]. An impedance tuning control for SBAR in inductive power transfer for electric vehicles is presented in [30]. However, impedance tuning algorithm is little complex.

In this work, CV performance of the WPT converter with LC/S compensation topology, which is providing good CC output, is evaluated. According to our current knowledge, [23] presents a design procedure only for CC operation. The CV regulation can be provided with frequency modulation (FM), however it causes high reactive power and conduction loss, resulting low efficiency. In [24], another design procedure of LC/S compensation to achieve CV operation is presented. This work realizes only CV operation. Besides, the CV output design procedure cannot achieve the ZPA operation for any load condition. Therefore, load-independent CC design procedure given in [23] is applied to LC/S compensation network. Then a controlled rectifier is used at the secondary side and phase shift modulation (PSM) control method, given in [29], is applied to the switches of the rectifier. Thus, CV operation of the LC/S compensation is provided at the constant operation frequency and so efficiency performance is improved. The operation of the

proposed WPT converter is validated by a simulation work with 2.5 kW output power and 450 V output voltage. The obtained efficiency values during CV operation are compared with frequency modulation (FM) control. The power loss distribution of the converter, for a certain load conditions, is also provided and compared with FM. According to obtained results, the maximum efficiency is obtained as 96.4% at full load condition.

2 Basic Principles of Secondary Side Controlled WPT Converter

The circuit schematic of the secondary side controlled WPT system using LC/S compensation is shown in Figure 1.

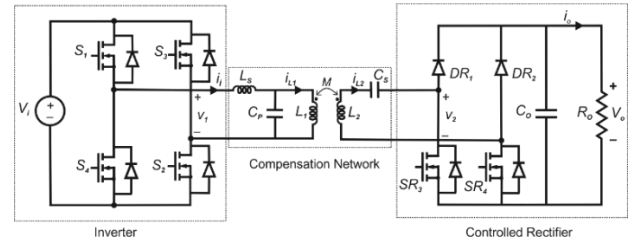


Figure 1. The proposed secondary side controlled WPT converter.

In the primary side, S_1 - S_4 switches constitute the inverter producing square wave alternate voltage, v_1 . V_1 is the dc input source feeding the inverter. L_s , C_p , C_s represent the LC/S compensation network. L_1 and L_2 represent the self-inductances of the primary coil and secondary coil. M is the mutual inductance between primary and secondary coil.

In the secondary side, bridgeless rectifier topology composed of DR_1 , DR_2 , SR_3 and SR_4 are used. DR_1 , DR_2 and antiparallel diodes of SR_3 and SR_4 operate as diode bridge and produce dc output voltage. C_o is used to filter the output of the rectifier. R_o is the load resistor.

2.1 Steady state analysis of compensation network

The sinusoidal equivalent circuit model of the proposed converter is given in Figure 2.

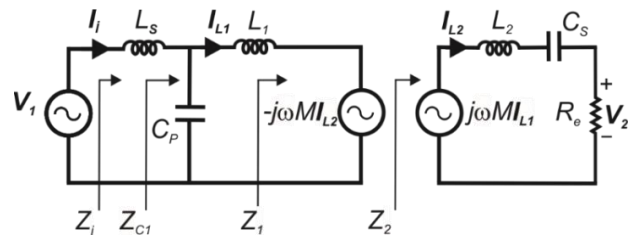


Figure 2. The equivalent circuit model of the secondary side controlled WPT converter.

V_1 phasor represents the first harmonic component of the square voltage produced by inverter. R_e represents the equivalent ac load resistor and ω represents the angular operation frequency. V_2 is the phasor voltage across the input of the rectifier, I_1 is the input current, I_{L1} and I_{L2} are the phasor currents of the primary and secondary coils, respectively. In the analysis of the converter, all circuit components are accepted as ideal.

Applying Kirchoff's voltage law to both side, voltage equation for each mesh is written as follows:

$$V_i = I_i \left(j\omega L_s + \frac{1}{j\omega C_p} \right) - I_{L1} \frac{1}{j\omega C_p} \quad (1)$$

$$-I_i \frac{1}{j\omega C_p} + I_{L1} j\omega L_1 + I_{L1} \left(\frac{1}{j\omega C_p} - j\omega M \right) = 0 \quad (2)$$

$$I_{L2} \left(j\omega L_2 + \frac{1}{j\omega C_s} + R_e \right) = j\omega M I_{L1} \quad (3)$$

The voltage across the load can be extracted as follows, based on the equivalent ac circuit given in Figure 2:

$$V_2 = V_1 \frac{jI_{L1} R_e Z_{C1} Z_i}{Z_i Z_2 (\omega L_1 - jZ_i)} \quad (4)$$

Where R_e can be defined as

$$R_e = \frac{V_2}{I_2} \quad (5)$$

Above equations, Z_i is the input impedance, Z_2 is the load impedance, Z_1 is the reflected impedance from the secondary side. They can be written as

$$Z_i = j\omega L_s + Z_{C1} \quad (6)$$

$$Z_2 = j \left(\omega L_2 - \frac{1}{\omega C_s} \right) + R_e \quad (7)$$

$$Z_1 = \frac{\omega^2 M^2}{Z_2} \quad (8)$$

Where Z_{C1} is the equivalent impedance of C_p , Z_1 and L_1 . It can be written as

$$Z_{C1} = \frac{Z_1 + j\omega L_1}{(1 - \omega^2 L_1 C_p) + jZ_i C_p} \quad (9)$$

2.2 Operation principles of controlled rectifier

In the operation of the rectifier, the output voltage and the power are controlled by the conduction angle, β , of the upper side diodes. The diode bridge is operating in the β . In the other times, secondary coil is short circuited by the conduction of SR_3 and antiparallel diode of SR_4 or by the conduction of SR_4 and antiparallel diode of SR_3 . In the positive half cycle of v_2 , SR_3 and antiparallel diode of SR_4 conduct the current while SR_4 and antiparallel diode of SR_3 are conducting it in negative half cycle of v_2 . During the short circuit operation of the secondary side, the input voltage of the rectifier becomes zero and no power is transferred to the load.

The power transferred to the load can be controlled to adjust the impedance of the input terminal of the rectifier. According to adjustment of the impedance, rectifier circuit can be operated in capacitive/inductive or resistive region. The current and voltage waveforms of the rectifier, based on the gate control signals of SR_3 and SR_4 , are given in Figure 3. If the conduction angle of the upper side diodes is set at the beginning of the half-cycle, inductive mode is operated as shown in Figure 3(a). Thus, the current is lag of the voltage. In the capacitive operation, the conduction angle is set at the end of half cycle as shown in Figure 3(b) and voltage is lag of the current. If the conduction angle is in the center of the current as shown in the Figure 3(c), resistive mode is operated. There is no phase shift between the voltage and the current waveforms. As shown in

Figure 3, according to the phase shift modulation (PSM), different operation regions are possible.

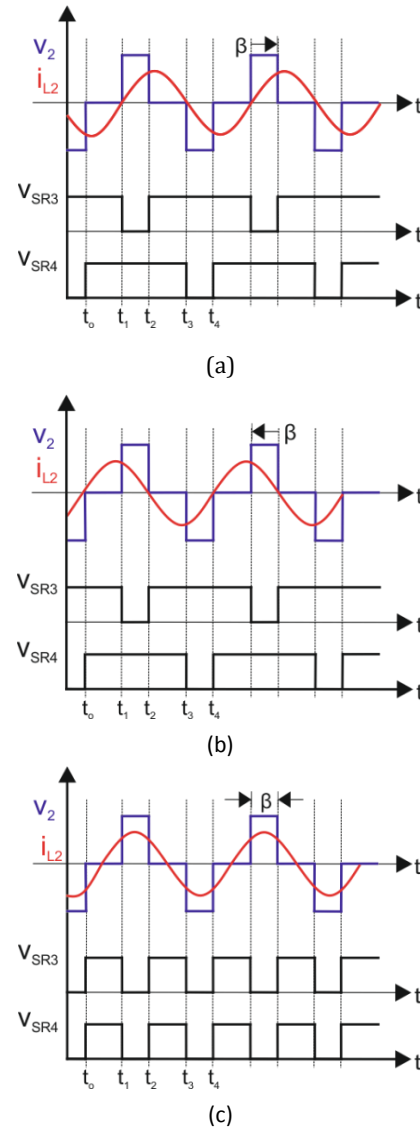


Figure 3. The operation condition of the controlled rectifier.
(a): Inductive operation. (b): Capacitive operation.
(c): Resistive operation.

The peak input voltage and the peak input current statements of the rectifier can be written, based on the first harmonic approximation (FHA) [29], as follows:

$$V_{2pk} = \frac{4V_o}{\pi} \sin\left(\frac{\beta}{2}\right) \quad (10)$$

$$I_{L2pk} = \frac{I_o \pi}{2 \sin\left(\frac{\beta}{2}\right)} \quad (11)$$

The equivalent load impedance expression can be given as follows [29]:

$$Z_{L-eq} = \frac{4}{\pi^2} R_o (1 - \cos\beta) \sin\left(\frac{\beta}{2}\right) e^{j\left(\frac{\pi}{2} - \frac{\beta}{2}\right)} \quad (12)$$

The load impedance has inductive characteristic during $0 \leq \beta \leq \pi$ while it has capacitive during $-\pi \leq \beta \leq 0$.

3 Performance evaluation for CV charging control mode of proposed WPT converter

In this section, efficiency performance of the proposed WPT converter, during the constant output voltage regulation, is evaluated. The operation conditions and the used circuit components belong to proposed WPT converter are summarized in Table 1 and Table 2, respectively. The components of the LC/S compensation topology are determined based on CC output design procedure given in [23]. Although CC design procedure is applied to the WPT converter, high efficiency CV operation is also provided by the use of the secondary side controlled rectifier in the proposed converter.

Table 1. The operation conditions of the proposed WPT converter.

P_o	2.5 kW
V_i	400 V
V_o	450 V
I_o	5.55 A
f_o	85 kHz
k	0.3

Table 2. The used circuit components of the proposed WPT converter.

Parameters	Values
$L_1 - L_2$	Coupled coils 310 μ H
L_S	Resonant inductor 310 μ H
C_P	Resonant capacitor 20.9 nF
C_S	Resonant capacitor 14 nF
$S_1 - S_4$	C3M0065090D / 900 V- 36 A $S_1 - S_4$ $t_r = 13$ ns, $t_f = 8$ ns
$DR_1 - DR_2$	C4D30120D / 1200 V- 43 A $DR_1 - DR_2$
$SR_3 - SR_4$	C3M0065090D / 900 V- 36 A $SR_3 - SR_4$ $t_r = 13$ ns, $t_f = 8$ ns

In the efficiency performance, firstly, power loss analysis is given for the circuit components, included in Figure 1. Then, simulation results and efficiency comparison results are provided as following.

3.1 The power loss analysis

The total power loss of the proposed WPT converter composed of losses come from the inverter, coupling coils, compensation circuit and the rectifier.

The switches of the inverter turn-on with ZVS so they have only turn-off switching losses and the conduction losses. They can be given as follows:

$$P_{sw-off} = \frac{1}{2} V_i I_{sw-off} t_f f_{sw} \quad (13)$$

$$P_{cond-sw} = I_{sw-RMS}^2 R_{DS-on} \quad (14)$$

Where, I_{sw-off} is the turn-off current, t_f is the falling time, R_{DS-on} is the turn-on resistance of the primary switches. I_{i-RMS} is the RMS value of the current flowing through the switches.

The coupling coils have only conduction losses due to no magnetic core material use in their design. The conduction losses of the coupling coils can be calculated as follows:

$$P_{cond-pr} = I_{L1-RMS}^2 R_{coil} \quad (15)$$

$$P_{cond-sc} = I_{L2-RMS}^2 R_{coil} \quad (16)$$

Where I_{L1-RMS} and I_{L2-RMS} represent the RMS value of the currents flowing through primary and secondary coils, respectively. The primary and secondary coils have same properties and geometry. R_{coil} represents the dc resistance of each coil. The ac resistance of the coupling coils is greatly reduced by the use of multiple litz wires.

The LC/S compensation circuit has the conduction and core losses of the L_S inductor. The dielectric losses of the C_S and C_P capacitors can be also taken into consideration. Their statements are given as follows:

$$P_{cond-L1} = I_{i-RMS}^2 R_{LS} \quad (17)$$

$$P_{CP,CS} = \left(\frac{I_{CP-RMS}^2}{C_P} + \frac{I_{CS-RMS}^2}{C_S} \right) \frac{\tan \delta}{\omega_{sw}} \quad (18)$$

Where I_{i-RMS} is the RMS current flowing through L_S . R_{LS} is the dc resistance of L_S inductor. The ac resistance of L_S is omitted due to the use of multiple litz wire. The RMS values of the ripple current flowing through capacitors are represented with I_{CP-RMS} and I_{CS-RMS} , respectively. The $\tan(\delta)$ represents the loss factor of the capacitors.

The turn-off and turn-on switching losses of the rectifier can be found according to equations given as follows:

$$P_{SR-off} = \frac{1}{2} V_i I_{SR-off} t_f f_{sw} \quad (19)$$

$$P_{SR-on} = \frac{1}{2} V_i I_{SR-on} t_r f_{sw} \quad (20)$$

Where, I_{SR-on} and I_{SR-off} represent the turn-on and turn-off currents of the switches of SBAR. t_r is the rising time of the current flowing through a switch.

The conduction loss of the SR_3 and SR_4 can be calculated as follows:

$$P_{cond-SR} = I_{L2-RMS}^2 R_{SR-on} (1 - \beta) f_{sw} \quad (21)$$

The conduction losses of the diodes in the rectifier circuit can be calculated as below:

$$P_{cond-diode} = I_{o-avg} V_{fw} f_{sw} \beta \quad (22)$$

Where, I_{o-avg} is the average current value of a diode and V_{fw} is the forward voltage drop. The reverse recovery power losses of the diodes can be omitted due to the use of Schottky diodes.

3.2 Simulation results

The constant voltage operation of the proposed WPT converter is tested with a simulation work. The components and operation conditions given in Table 1 and 2 are used in the simulation work. In the simulation study, the output voltage is measured and compared to the reference voltage. The error between the reference and measured values of output voltage is entered into the input of PI controller. The output of PI controller gives the appropriate β values according to load variation. Figure 4 provides the voltage and current waveforms obtained from the output of the inverter ($v_1 - i_i$) and the input of the rectifier ($v_2 - i_2$) at full load condition. There is no phase shift is observed between $v_2 - i_2$ and $v_1 - i_i$. Same waveforms, at 50% and 25% load conditions, are given in Figure 5 and Figure 6, respectively. Although the phase shift is observed between voltage and current waveforms, the output voltage regulation is provided with no need of the operation frequency change. As

shown in Figure 7, the output voltage regulation is achieved at 450 V while the load is changed from full to 25% and the operation frequency is 85 kHz. The battery behavior is represented by a load resistor in the simulation work. Although, the variation of the output voltage across a fixed resistor will be different from the variation during battery charging, the β can be adjusted with the suitable value for the battery charging. Even if the beta values are little change in the real battery, the system performance will not make much difference in terms of the output voltage regulation. The new beta will compensate for the difference between battery charge and pure resistance.

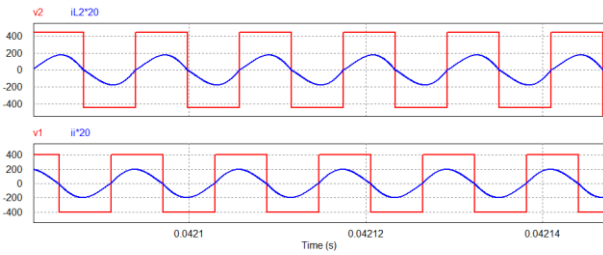


Figure 4. The voltage and current waveforms at the output of the inverter and the input of the rectifier, at full load condition. $V_o=450$ V, $I_o=5.55$ A, $f_o=85$ kHz.

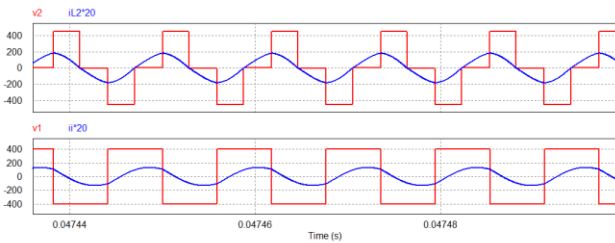


Figure 5. The voltage and current waveforms at the output of the inverter and the input of the rectifier, at 50% load condition. $V_o=450$ V, $I_o=2.77$ A, $f_o=85$ kHz.

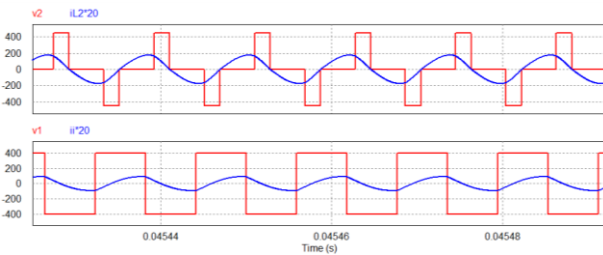


Figure 6. The voltage and current waveforms at the output of the inverter and the input of the rectifier, at 25% load condition. $V_o=450$ V, $I_o=1.39$ A, $f_o=85$ kHz.

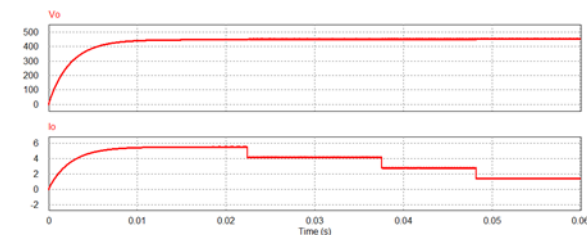


Figure 7. The output voltage regulation while the load changes from full to 25%. $f_{sw}=85$ kHz, $V_{in}=400$ V.

3.3 Efficiency performance

The efficiency performance of the proposed WPT converter is evaluated based on simulation work. In the evaluation, PSM control and frequency modulation (FM) control are separately applied to the proposed converter to compare their performance in CV charging control mode. In the FM control, the control of the primary side achieves the output voltage regulation, the secondary side does not need to be controlled. Therefore, SBAR operates as conventional diode bridge during the FM control. The switches of the SBAR are controlled while the PSM control is performing. The efficiency values during the CV charging control are extracted for each control method. The obtained values as function of the load variation are given in Figure 8.

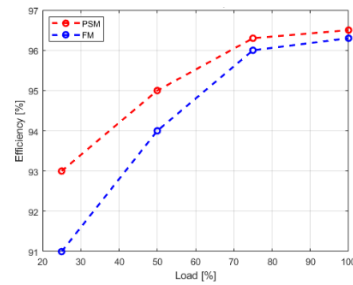
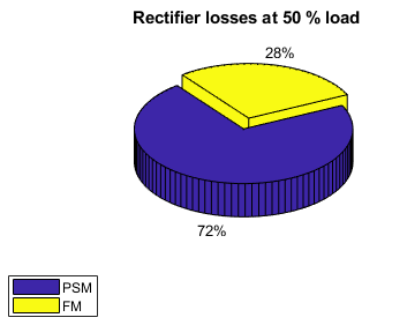
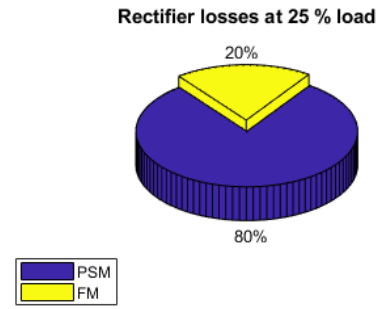


Figure 8. The efficiency comparison of the proposed converter based on PSM and FM control methods.

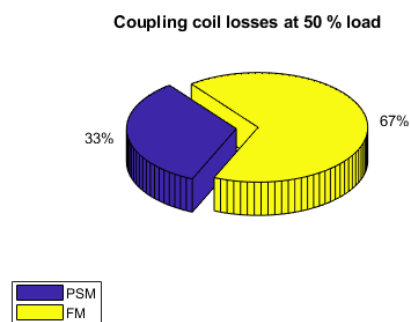
The PSM method has higher efficiency values compared to the FM. In the frequency modulation, frequency range is changed between 88.4 kHz and 90.2 kHz to regulate the output voltage while large reactive power drives to the power source. In PSM, the eliminating of the switching frequency variation decreases reactive power to the power source. Thus, large conduction occurring in FM is decreased with applying of PSM control. Besides, turn-off switching losses of the inverter switches at high switching frequencies, required for output voltage regulation in FM, is also decreased. Therefore, the improvement of the efficiency is much more significant at the light load conditions since the switching losses are dominated in the low power rates. In Figure 9 and Figure 10, the power loss comparison of the applied control methods, occurring at the different power stages of the proposed converter, are given with pie charts for the 50% and 25% load conditions. Figure 9(a)-(d) and Figure 10(a)-(d) show the power loss comparison of rectifier, coupling coils, inverter and LC/S compensation topology, respectively. In Figure 9(a), FM control has lower power loss since the rectifier works as diode bridge and the current flows through the antiparallel diodes of SR_3 and SR_4 . Thus, only conduction losses of the rectifier diodes are included in pie chart. PSM control has bigger percent due to the switching losses of the SR_3 and SR_4 . In Figure 9 (b), the power loss of the coupling coils with FM control is higher than the PSM because the frequency variation causes to larger reactive power which results in high conduction losses in the coil windings. Similarly, as shown in Figure 9(c), FM control causes high conduction losses at the inverter stage. In Figure 9 (d), FM has big percent due to the increased conduction losses of the L_s inductor in the compensation topology. Similar results are also obtained for 25% load condition as shown in Figure 10 (a)-(d). According to these results, the advantage of the PSM control method is prominent especially at the light load conditions compared to FM control.



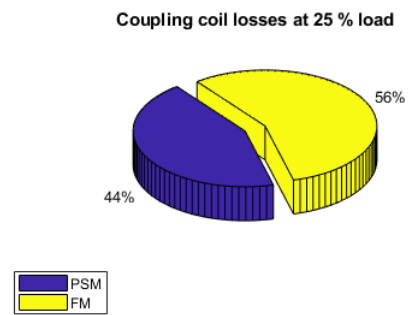
(a)



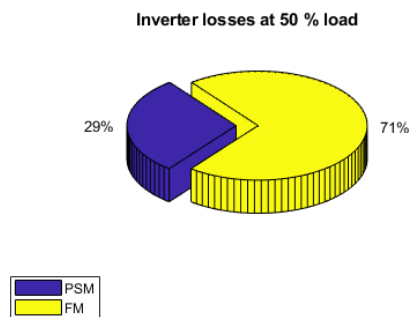
(a)



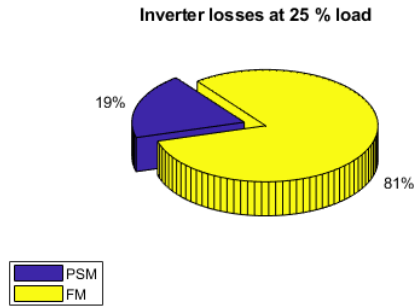
(b)



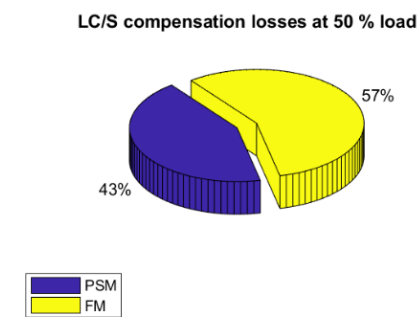
(b)



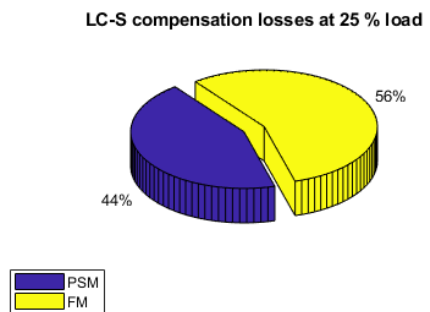
(c)



(c)



(d)



(d)

Figure 9. The power loss comparison of PSM and FM control methods for 50% load condition in the different power stages of the proposed converter.

Figure 10. The power loss comparison of PSM and FM control methods for 25% load condition in the different power stages of the proposed converter.

4 Conclusions

In this work, constant output voltage control of a wireless power transfer (WPT) converter is evaluated based on efficiency. In the design of the proposed converter, LC/S compensation topology which has perfect constant output current characteristic is used. The constant output voltage regulation of the converter is improved applying PSM control to the switches of the rectifier. The output voltage regulation is provided at 85 kHz operation frequency in a wide load range, as independent of the primary side. The maximum efficiency is obtained 96.4% at full load condition. The efficiency of the converter is also compared to FM control as function of the load condition. According to 25% load condition, 2% efficiency improvement is provided compared to conventional frequency modulation, during CV regulation.

5 Author contribution statements

Veli YENİL put contribution in literature searching, analyzing of the proposed WPT system. He also carried out the simulation work and efficiency performance of the proposed WPT system. Sevilyay ÇETİN put contribution in the managing all stages in the paper. This work is supported by Pamukkale University under grant number 2020FEBE034.

6 Ethics committee approval and conflict of interest statement

There is no need to obtain permission from the ethics committee for the article prepared.

There is no conflict of interest with any person / institution in the article prepared.

7 References

- [1] Li S, Mi CC. "Wireless power transfer for electric vehicle applications". *IEEE Journal Emerging and Selected Topics in Power Electronics*, 3(1), 4-17, 2015.
- [2] Miller JM, Jones PT, Li JM, Onar OC. "ORNL experience and challenges facing dynamic wireless power charging of EV's". *IEEE Circuits and Systems Magazine*, 15(2), 40-53, 2015.
- [3] Xiao C, Cheng D, Wei K. "An LCC-C compensated wireless charging system for implantable cardiac pacemakers: Theory, experiment, and safety evaluation". *IEEE Transactions on Power Electronics*, 33(6), 4894-4905, 2018.
- [4] Chen M, Rincón-Mora GA. "Accurate, compact and power-efficient li-ion battery charger circuit". *IEEE Transactions on Circuits Systems II: Express Briefs*, 53(11), 1180-1184, 2006.
- [5] Dearborn S. "Charging li-ion batteries for maximum run times". *Power Electronics Technology Magazine*, 31(4), 40-49, 2005.
- [6] Andrea D. "Battery Management Systems for Large Lithium-Ion Battery Packs". 1st ed. Boston, MA, USA: Artech House, 2010.
- [7] Covic GA, Boys JT. "Modern trends in inductive power transfer for transportation applications". *IEEE Journal of Emerging and Selected Topics in Power Electronics*, 1(1), 28-41, 2013.
- [8] Zhou W, Ma H. "Design considerations of compensation topologies in ICPT system". *APEC 07-Twenty-Second Annual IEEE Applied Power Electronics Conference and Exposition*, Anaheim, CA, USA, 25 February-1 March 2007.
- [9] Sallán J, Villa JL, Llombart A, Sanz JF. "Optimal design of ICPT systems applied to electric vehicle battery charge". *IEEE Transactions on Industrial Electronics*, 56(6), 2140-2149, 2009.
- [10] Villa JL, Sallán J, Llombart A, Sanz JF. "Design of a high frequency inductively coupled power transfer system for electric vehicle battery charge". *Applied Energy*, 86(3), 355-363, 2009.
- [11] Wang CS, Stielau OH, Covic GA. "Design considerations for a contactless electric vehicle battery charger". *IEEE Transactions on Power Electronics*, 52(5), 1308-1314, 2005.
- [12] Hou J, Chen Q, Wong SC, Tse CK, Ruan X. "Analysis and control of series/series-parallel compensated resonant converter for contactless power transfer". *IEEE Journal of Emerging and Selected Topics in Power Electronics*, 3(1), 124-136, 2015.
- [13] Zhang W, Wong SC, Chi KT, Chen Q. "Load-independent duality of current and voltage outputs of a series or parallel compensated inductive power transfer converter with optimized efficiency". *IEEE Journal of Emerging and Selected Topics in Power Electronics*, 3(1), 137-146, 2015.
- [14] Qu X, Han H, Wong SC, Chi KT, Chen W. "Hybrid IPT topologies with constant-current or constant-voltage output for battery charging applications". *IEEE Transactions on Power Electronics*, 30(11), 6329-6337, 2015.
- [15] Chen Q, Wong SC, Chi KT, Ruan X. "Analysis, design, and control of a transcutaneous power regulator for artificial hearts". *IEEE Transactions on Biomedical Circuit and System*, 3(1), 23-31, 2009.
- [16] Zheng C, Lai JS, Chen R, Faraci WE, Zahid ZU, Gu B, Zhang L, Lisi G, Anderson D. "High-efficiency contactless power transfer system for electric vehicle battery charging application". *IEEE Journal Emerging and Selected Topics in Power Electronics*, 3(1), 65-74, 2015.
- [17] Vu VB, Tran DH, Choi W. "Implementation of the constant current and constant voltage charge of inductive power transfer systems with the double-sided LCC compensation topology for electric vehicle battery charge applications". *IEEE Transactions on Power Electronics*, 33(9), 7398-7410, 2018.
- [18] Wang CS, Covic GA, Stielau OH. "Investigating an LCL load resonant inverter for inductive power transfer applications". *IEEE Transactions on Power Electronics*, 19(4), 995-1002, 2004.
- [19] Voglitsis D, Todorčević T, Prasanth V, Bauer P. "Loss model and control stability of bidirectional LCL-IPT system". *4th International Electric Drives Production Conference (EDPC)*, Nuremberg, Germany, 30 September-1 October 2014.
- [20] Keeling NA, Covic GA, Boys JT. "A unity-power-factor IPT pickup for high-power applications". *IEEE Transactions on Industrial Electronics*, 57(2), 744-751, 2010.
- [21] Pantic Z, Bai S, Lukic SM. "ZCS LCC-compensated resonant inverter for inductive-power-transfer application". *IEEE Transactions on Industrial Electronics*, 58(8), 3500-3510, 2011.
- [22] Li S, Li W, Deng J, Nguyen TD, Mi CC. "A double-sided LCC compensation network and its tuning method for wireless power transfer". *IEEE Transactions on Vehicular Technology*, 64(6), 2261-2273, 2015.
- [23] Wang Y, Yao Y, Liu X, Xu D, Cai L. "LC/S compensation topology and coil design technique for wireless power

- transfer". *IEEE Transactions on Power Electronics*, 33(3), 2007-2024, 2018.
- [24] Yao Y, Wang Y, Liu X, Xu D. "Analysis, design, and optimization of LC/S compensation topology with excellent load-independent voltage output for inductive power transfer". *IEEE Transactions on Transportation Electrification*, 4(3), 767-777, 2018.
- [25] Cetin S, Yenil V. "Performance evaluation of constant current and constant voltage charge control modes of an inductive power transfer circuit with double-sided inductor-capacitor-capacitor and inductor-capacitor/series compensations for electrical vehicle battery charge applications". *Transactions of the Institute of Measurement and Control*, 43(8), 1710-1721, 2021.
- [26] Kato M, Imura T, Hori Y. "Study on maximize efficiency by secondary side control using DC-DC converter in wireless power transfer via magnetic resonant coupling". *World Electric Vehicle Symposium and Exhibition (EVS27)*, Barcelona, Spain, 17-20 November 2013.
- [27] Colak K, Bojarski M, Asa E, Czarkowski D. "A constant resistance analysis and control of cascaded buck and boost converter for wireless EV chargers". *IEEE 2015 Applied Power Electronics Conference and Exposition (APEC)*, Charlotte, NC, USA, 15-19 March 2015.
- [28] Diekhans T, De Doncker RW. "A dual-side controlled inductive power transfer system optimized for large coupling factor variations and partial load". *IEEE Transactions on Power Electronics*, 30(11), 6320-6328, 2015.
- [29] Colak K, Asa E, Bojarski M, Czarkowski D, Onar OC. "A novel phase-shift control of semibridgeless active rectifier for wireless power transfer". *IEEE Transactions on Power Electronics*, 30(11), 6288-6297, 2015.
- [30] Ann S, Lee BK. "Analysis of Impedance tuning control and synchronous switching technique for a semibridgeless active rectifier in inductive power transfer systems for electric vehicles". *IEEE Transactions on Power Electronics*, 36(8), 8786-8798, 2021.